Articles

Transient Kinetic Analysis of Adenosine 5′-Triphosphate Binding-Induced Conformational Changes in the Allosteric Chaperonin GroEL†

Ofer Yifrach and Amnon Horovitz*

Department of Structural Biology, Weizmann Institute of Science, Rehovot 76100, Israel

Received February 17, 1998; Revised Manuscript Received March 20, 1998

ABSTRACT: GroEL with an intrinsic fluorescent probe was generated by introducing the mutation Phe44 → Trp. Different concentrations of ATP were rapidly mixed with GroEL containing this mutation, and the time-resolved change in fluorescence emission, upon excitation at 280 nm, was followed. Three kinetic phases were observed: a fast phase with a large amplitude and two slower phases with small amplitudes. The phases were assigned by (i) determining their dependence on ATP concentration; (ii) measuring their sensitivity to the mutation Arg197 → Ala, which decreases cooperativity in ATP binding; and (iii) by carrying out mixing experiments of GroEL also with ADP, ATPγS, and ATP without K^+. The apparent rate constant corresponding to the fast phase displays a bi-sigmoidal dependence on ATP concentration with Hill coefficients that are strikingly similar to those determined in steady-state experiments. This phase, which reflects ATP-induced conformational changes, is sensitive to the mutation Arg197 → Ala in a manner that parallels steady-state experiments. The rate of conformational change in the presence of ATP is >100 sec^{-1}, which is fast relative to most protein folding rates, whereas in the absence of ATP it is ~ 0.7 s^{-1}. The second phase reflects the transition from an ATP-bound state of GroEL to an ADP-bound state. The third phase, with the smallest amplitude, reflects release of residual contaminants. The results in this study are found to be consistent with the nested model for cooperativity in ATP binding by GroEL [Yifrach, O., and Horovitz, A. (1995) *Biochemistry 34*, 5303−5308].

The chaperonin GroEL from *Escherichia coli* consists of 14 identical subunits that form two stacked heptameric rings with a central cavity (*1*, *2*). It facilitates protein folding in vivo and in vitro in an ATP-regulated manner (for reviews see, for example, refs *3*−*5*). GroEL has 14 ATP binding sites and a weak K^+-dependent ATPase activity, which is cooperative with respect to ATP (*6*−*8*) and K^+ ions (*9*). A nested model for cooperativity in ATP hydrolysis by GroEL has been proposed in which there are two levels of allostery: one within each ring and the second between rings (*10*). In the first level, in accordance with the Monod−Wyman−Changeux (MWC)[1] representation (*11*), each heptameric ring is in equilibrium between two states: a tense (**T**) state, with low affinity for ATP and high affinity for nonfolded proteins, and a relaxed (**R**) state, with high affinity for ATP and low affinity for nonfolded proteins (*12*). A second level of allostery is between the rings of the GroEL particle which undergoes sequential Koshland−Némethy−Filmer (KNF)-type transitions from the **TT** state via the **TR** state to the **RR** state (*13*). In this model (*11*), there is positive cooperativity within rings and negative cooperativity between rings. Owing to negative cooperativity between rings, the transition of the second ring from the **T** to the **R** state (i.e., the transition of the GroEL particle from the **TR** state to the **RR** state) is observed only at higher concentrations of ATP or at low concentrations of ATP in the presence of GroES (*14*, *15*). Recent electron microscopy studies (*16*−*18*) have provided structural evidence in support of the nested allosteric model.

In this study, we have introduced the mutation Phe44 → Trp into GroEL (which has no tryptophan residues) to follow the binding of ATP to GroEL and the resulting conformational changes by monitoring of the time-resolved changes in fluorescence. Information about rate constants of elementary steps of ATP binding and conformational changes in GroEL is required for a full understanding of GroEL's mechanism of action and is also of interest owing to the unusual allosteric properties of the GroE system. The results of the transient kinetic analysis support the nested allosteric model which was initially proposed on the basis of steady-state kinetic studies (*10*).

† This work was supported by The Israel Science Foundation administered by The Israel Academy of Sciences and Humanities and by the Henri Gutwirth Fund. A.H. is an incumbent of the Robert Edward and Roselyn Rich Manson Career Development Chair.

* Author to whom correspondence should be addressed (fax ++972 8 9344188; telephone ++972 8 9343399; e-mail csamnon@weizmann.weizmann.ac.il).

[1] Abbreviations: DTT, dithiothreitol; EDTA, ethylenediaminetetraacetic acid; KNF, Koshland, Némethy, and Filmer; MES, 2-(*N*-morpholino)ethanesulfonic acid; MWC, Monod, Wyman, and Changeux.

S0006-2960(98)00370-5 CCC: $15.00
Published on Web 04/30/1998

EXPERIMENTAL PROCEDURES

Materials. Radiochemicals and the Sculptor RPN 1526 mutagenesis kit were purchased from Amersham International. All other reagents were from Sigma or Aldrich.

Molecular Biology and Biochemical Methods. Single-stranded DNA of the plasmid pOA containing the gene for wild-type GroEL or the Arg197 → Ala GroEL mutant was obtained by infecting *E. coli* TG2 cells harboring the appropriate plasmid with M13KO7 helper-phage (Pharmacia, Uppsala, Sweden). The Phe44 → Trp single mutant and the Phe44 → Trp; Arg197 → Ala double mutant were generated as before (*19*) using the appropriate single-stranded DNA and the mutagenic oligonucleotide (Phe44 → Trp): 5′-GATGGTCGGTGCACCC*C*AAGATTTATCCAGAAC-3′. An asterisk follows the mismatched bases. Protein expression was carried out as before (*19*), and purification of GroEL was achieved as described earlier (*20*) with some modification (Matthew Todd and George Lorimer, personal communication). GroEL-enriched fractions after gel filtration were combined, applied to a Mono-Q HR 5/5 column, and eluted using a linear gradient from 0.15 to 0.35 M NaCl (35 min, 1 mL/min) in 50 mM MES buffer (pH 6.0) containing 1 mM EDTA, 1 mM DTT, and 25% methanol. GroEL purified in this manner contained <1 mol tryptophan/mol of GroEL oligomer. The ATPase activity of GroEL was measured as described by Viitanen et al. (*21*) with some modifications (*19*).

Fluorescence Emission Spectra Measurements. An SLM-Aminco 8100 spectrofluorometer was used for the measurements. The excitation wavelength was 280 nm with a bandpass of 4 nm. A frozen aliquot of wild-type GroEL or the Phe44 → Trp mutant (125 nM) was thawed and incubated for 20 min at 25 °C in 50 mM Tris-HCl buffer containing 10 mM $MgCl_2$, 10 mM KCl, and 1 mM DTT (pH 7.5) before data collection. Data collection in the presence of ATP was made 5 min after its addition.

Stopped-Flow Experiments. Binding of ATP to GroEL was initiated by rapid mixing of equal volumes of different concentrations of nucleotide and the appropriate GroEL mutant using an Applied Photophysics SX.17MV stopped-flow apparatus. The reactions were carried out at 25 °C in 50 mM Tris-HCl buffer containing 10 mM $MgCl_2$, 10 mM KCl, and 1 mM DTT (pH 7.5). The final GroEL concentration was 0.25 μM. Binding of ATP to GroEL was followed by excitation at 280 nm and monitoring the tryptophan fluorescence emission at wavelengths longer than 320 nm using a cutoff filter. A 1 cm path length was used, and both the entrance and exit monochromator slit widths were set to 7 nm.

Data Analysis. Initial velocities of ATP hydrolysis as a function of ATP concentration were fitted to the previously derived equation for a three-state nested allosteric model (*10*)

$$V_0 = [0.5V_{max(1)}L_1([S]/K_R)(1 + [S]/K_R)^{N-1} + V_{max(2)}L_1L_2([S]/K_R)(1 + [S]/K_R)^{2N-1}]/[1 + L_1(1 + [S]/K_R)^N + L_1L_2(1 + [S]/K_R)^{2N}] \quad (1)$$

where L_1 and L_2 are the respective apparent allosteric constants for the transitions **TT** → **TR** and **TR** → **RR**, V_0 is the initial rate of ATP hydrolysis, $V_{max(1)}$ and $V_{max(2)}$ are the respective maximal initial rates of ATP hydrolysis of the **TR** and **RR** states, and K_R is the dissociation constant of ATP for rings in the **R** state.

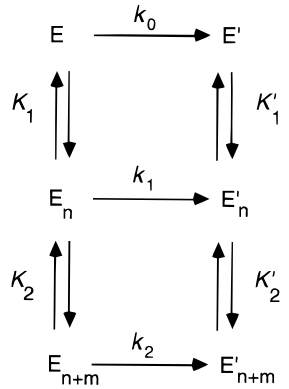

FIGURE 1: Scheme for different states of GroEL considered in the kinetic analysis. Two sequential reactions of ATP binding to GroEL (E) take place in which *n* and then *m* molecules of ATP bind in an all-or-none fashion with apparent dissociation constants K_1 and K_2, respectively. These two reactions correspond to binding of ATP first to one ring of GroEL and then to the other ring. Binding of ATP induces a conformational change in GroEL, which is designated by a prime (′). The forward rate constants of the conformational changes E → E′, E_n → E′$_n$, and E_{n+m} → E′$_{n+m}$ are designated k_0, k_1, and k_2, respectively.

Steady-state analysis of ATP binding and hydrolysis by GroEL using eq 1 takes into account all of the possible ATP-bound states of GroEL in the **TT**, **TR**, and **RR** conformations (*10*). This is not possible in the case of transient kinetic analysis. To simplify the transient kinetic analysis, we therefore consider a scheme (Figure 1) in which it is assumed (as in the original formulation of the Hill equation) that only unliganded or fully liganded states of the two rings of GroEL (E) exist. Binding of ATP induces a conformational change in GroEL, which is designated by a prime (′). Following Hammes and Schimmel (*22*), we also assume that ATP binding occurs much more rapidly than the ATP-induced conformational changes, so that we can, therefore, define an observed forward rate constant for conformational changes, k_{obs}, as follows:

$$k_{obs} = \frac{k_0 + k_1([S]/K_1)^n + k_2([S]/K_1)^n([S]/K_2)^m}{1 + ([S]/K_1)^n + ([S]/K_1)^n([S]/K_2)^m} \quad (2)$$

In eq 2, k_0, k_1, and k_2 are the forward rate constants for the conformational changes E → E′, E_n → E′$_n$, and E_{n+m} → E′$_{n+m}$, [S] is the substrate (ATP) concentration, K_1 and K_2 are the respective apparent dissociation equilibrium constants of ATP for the first and second rings, and *n* and *m* are the respective Hill coefficients for ATP binding to the first and second rings. The values of the Hill coefficients, which correspond in the original formulation of the Hill equation to the total number of sites in each ring, are here only a measure of the extent of cooperativity in each ring.

Data fitting was carried out using Kaleidagraph [version 2.1, Synergy Software (PCS Inc.)]. Estimates of parameters (± standard errors) are reported.

RESULTS

Construction and Characterization of the Phe44 → Trp GroEL Mutant. Multiple-sequence alignment of various

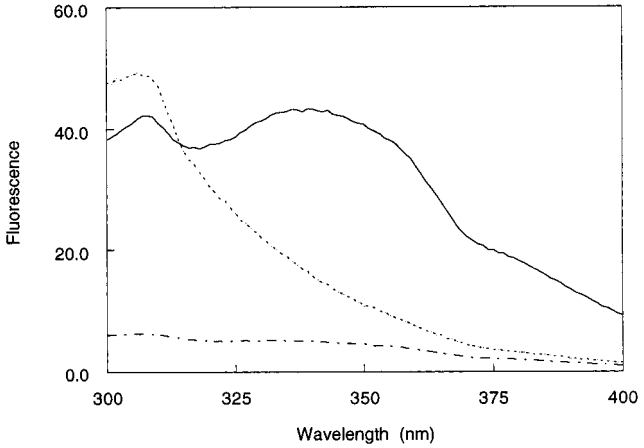

FIGURE 2: Fluorescence emission spectra of wild-type GroEL and the Phe44 → Trp mutant in the absence and presence of ATP. Fluorescence emission spectra of wild-type GroEL (dotted line···) and the Phe44 → Trp GroEL mutant without (continuous line—) and with 1 mM ATP (dashed line—·—) are shown. The spectra were recorded in 50 mM Tris-HCl buffer containing 10 mM $MgCl_2$, 10 mM KCl, and 1 mM DTT (pH 7.5) at 25 °C using an excitation wavelength of 280 nm with a band-pass of 4 nm. The oligomer concentration of wild-type GroEL and the Phe44 → Trp mutant was 125 nM.

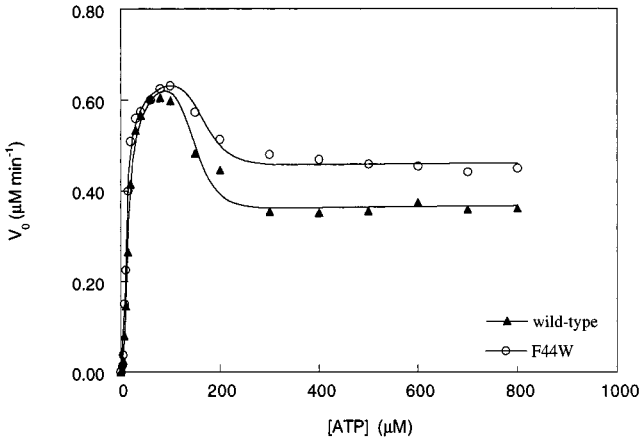

FIGURE 3: Initial velocities of ATP hydrolysis by wild-type GroEL and the Phe44 → Trp mutant at different concentrations of ATP. The reactions were carried out in 50 mM Tris-HCl buffer containing 10 mM $MgCl_2$, 10 mM KCl, and 1 mM DTT (pH 7.5) at 25 °C as previously described (*19*). The oligomer concentration of GroEL is 25 nM. The data were fitted to eq 1 (see Experimental Procedures).

GroEL homologues revealed that residue Phe44 is relatively conserved except in some organisms where it is replaced by tryptophan. This residue is part of an antiparallel β-loop that projects from the body of the equatorial domain toward the inner surface of the adjacent subunit. Examination of the structure showed that Phe44 does not interact with any neighboring residues (*1*). This residue was, therefore, replaced by tryptophan using site-directed mutagenesis. Fluorescence emission spectra of the Phe44 → Trp GroEL mutant, upon excitation at 280 nm, show a peak of emission at 345 nm due to tryptophan residues that is quenched in the presence of ATP (Figure 2). This peak is absent in the spectrum of wild-type GroEL. Initial velocities of ATP hydrolysis by the Phe44 → Trp mutant were measured at different concentrations of ATP (Figure 3). Two allosteric transitions are observed: one at relatively low ATP concentrations from the **TT** state to the **TR** state and the second at higher concentrations of ATP from the **TR** state to the **RR** state, which has a lower k_{cat} of ATP hydrolysis (*10*). The data were fitted to eq 1. The values of the allosteric constant, L_1, the ATP dissociation constant (K_R), and the k_{cat} of the **TR** state were found to be 2.0 (±1.0) × 10^{-3}, 7.6 (±0.2) μM, and 0.065 (±0.001) s^{-1}, respectively. These values are essentially identical to those determined for wild-type GroEL (*10*). The values of the allosteric constant, L_2, and k_{cat} of the **RR** state were found to be 6.0 (±1.2) × 10^{-10} and 0.022 (±0.0002) s^{-1}, respectively. These values differ somewhat from the values of 6.0 (±3.2) × 10^{-9} and 0.017 (±0.0004) s^{-1} for L_2 and k_{cat} determined for wild-type GroEL. Overall, the mutation Phe44 → Trp was found to have little effect on the rates of ATP hydrolysis by GroEL and on its allosteric properties with respect to ATP, in particular, with regard to the first allosteric transition (Figure 3). The engineered tryptophan residue at position 44 is, therefore, an excellent probe for studying the dynamics of GroEL−ATP interactions.

Kinetics of ATP Association to GroEL. Equal volumes of different concentrations of ATP and GroEL were rapidly mixed, and the time-resolved change in fluorescence emission upon excitation at 280 nm was followed. Ten or more traces (each with 2000 data points) were collected and averaged for each concentration of ATP. A typical trace corresponding to the mixing of Phe44 → Trp mutant GroEL with 1 mM ATP is shown in Figure 4A. It can be seen that an initial quenching phase is followed by a rise in the fluorescence. A similar trend was observed in all of the mixing experiments regardless of the GroEL mutant or ATP concentration used. The data were fitted to a triple-exponential equation with a floating end-point yielding estimates for the amplitudes and apparent rate constants. Owing to inner-filter effects, an analysis of the amplitudes is not presented in this paper. Plots of residuals with random deviations about zero were obtained for all of the kinetic traces (Figure 4B). Single- and double-exponential equations failed to fit the data as indicated by residuals with nonrandom deviations about zero (Figure 4C). The three kinetic phases were assigned by (i) determining their dependence on ATP concentration; (ii) measuring their sensitivity to the mutation Arg197 → Ala, which decreases cooperativity in ATP binding (*20*); and (iii) carrying out mixing experiments of GroEL with ADP, ATPγS, and ATP without K^+ as described below.

ATP Binding-Induced Conformational Changes. The observed rate constant corresponding to the first and fastest kinetic phase is found to have a bi-sigmoidal dependence on ATP concentration (Figure 5). The data were fitted to eq 2, which was derived by assuming that ATP binding occurs much more rapidly than the binding-induced conformational changes as often observed experimentally (*23*). The results of the data fitting are presented in Table 1. The values of k_0 were determined by linear extrapolation to zero of the data for k_{obs} at very low ATP concentrations, where k_{obs} is ATP concentration-independent. These values were used as constants in the data fitting. It may be seen that $k_2 > k_1 > k_0$ for both the Phe44 → Trp single mutant and the Phe44 → Trp; Arg197 → Ala double mutant, indicating that bound ATP accelerates the conformational switch. The values of the Hill coefficient, n, for the first transition of the Phe44 → Trp single mutant and the Phe44 → Trp; Arg197 → Ala

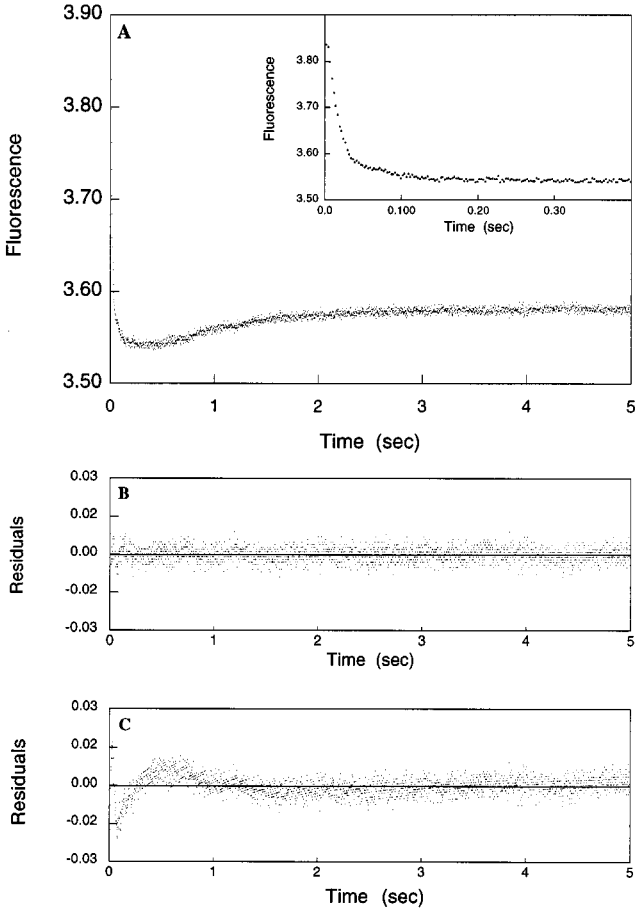

FIGURE 4: Time-resolved change in fluorescence emission upon rapid mixing of ATP and GroEL. Equal volumes of 1 mM ATP and 250 nM Phe44 → Trp mutant GroEL were rapidly mixed, and the time-resolved change in fluorescence emission upon excitation at 280 nm was followed (A). Plots of residuals with random deviations about zero were obtained by fitting the data to a triple-exponential equation (B). Single- and double-exponential equations failed to fit the data as indicated by residuals with nonrandom deviations about zero shown in panel C for a fit to a double-exponential equation. For further details see Experimental Procedures.

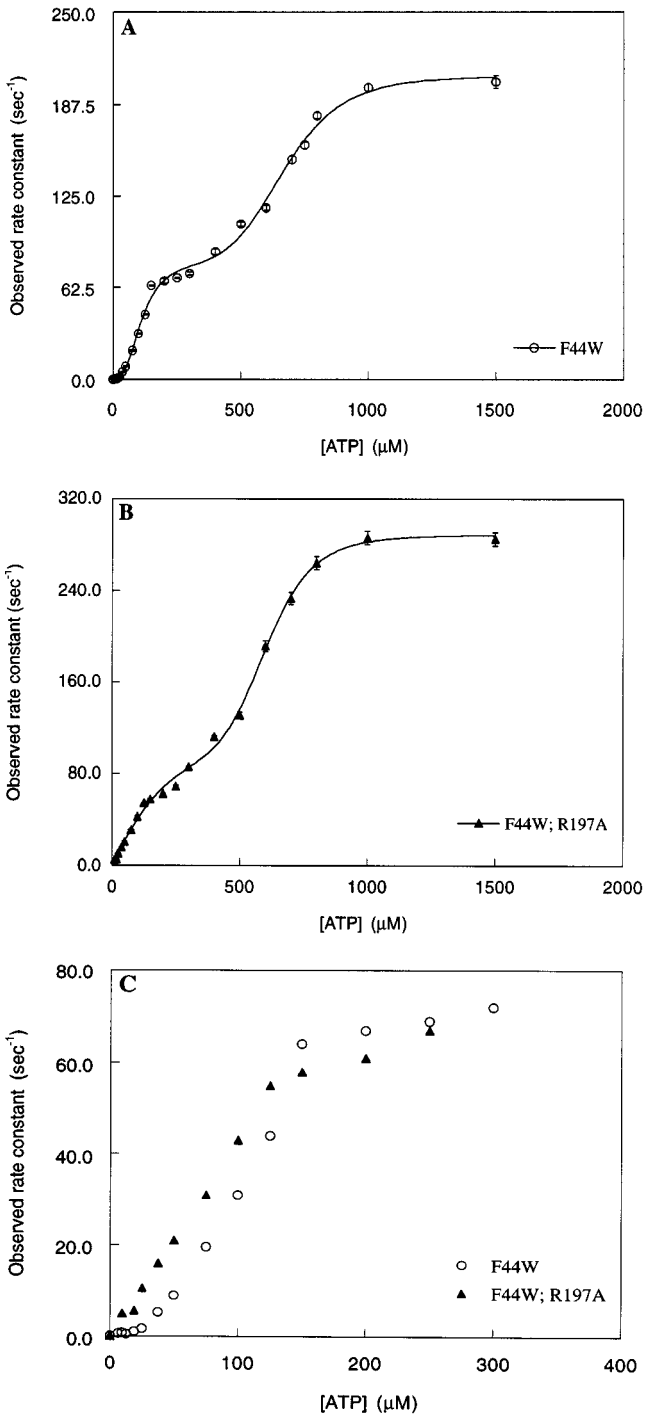

FIGURE 5: Observed rate constant corresponding to the fast kinetic phase, which reflects conformational changes in GroEL as a function of ATP concentration. The data for the Phe44 → Trp single mutant (A) and the Phe44 → Trp, Arg197 → Ala double mutant (B) were fitted to eq 2. The data for the two mutants at ATP concentrations below 300 μM are shown in panel C. The results of the data fitting are given in Table 1. For further details see Experimental Procedures.

double mutant are 2.85 (± 0.46) and 1.37 (± 0.25), respectively (Figure 5C). These values are strikingly similar to the values of 2.75 (± 0.12) and ~1 obtained for wild-type GroEL and the Arg197 → Ala mutant in steady-state kinetic experiments under the same conditions (*10*). The values of the Hill coefficient, *m*, for the second transition of the Phe44 → Trp single mutant and the Phe44 → Trp; Arg197 → Ala double mutant are equal to ~7 and, thus, are significantly higher than those of the Hill coefficient for the first transition. In the case of both mutants, $K_1 < K_2$, but because these dissociation constants are apparent, their values cannot be directly compared to values determined from analysis of steady-state experiments using the nested model.

The Second Phase Reflects ATP Hydrolysis. The second phase, which is reflected by a rise in the fluorescence emission, is not observed when the Phe44 → Trp GroEL mutant is mixed with ADP or ATPγS (Figure 6). It is also not observed when the Phe44 → Trp GroEL mutant is mixed with ATP in the absence of K^+, which inhibits ATP hydrolysis (*9*, *21*). In the absence of this phase, good fits of the data to a double-exponential equation are obtained (not shown). The rate constant corresponding to this phase is ~1 s^{-1}, and it is ATP concentration-independent (not shown). We, therefore, conclude that the second phase, which is ATP hydrolysis-dependent, reflects the transition from an ATP-bound state of GroEL to an ADP-bound state with lower fluorescence. This conclusion is supported also by evidence from other laboratories which suggests that ADP stabilizes a distinct state. First, reported values of Hill coefficients for ADP binding to GroEL are lower than those

Table 1: Kinetic Parameters for ATP Binding to the GroEL Phe44 → Trp Single Mutant and the Phe44 → Trp; Arg197 → Ala Double Mutant[a]

GroEL	k_0 (s^{-1})	k_1 (s^{-1})	k_2 (s^{-1})	K_1 (μM)	K_2 (μM)	n	m
F44W	0.7 (±0.2)	80 (±5)	207 (±4)	113 (±8)	671 (±15)	2.85 (±0.46)	5.89 (±0.70)
F44W, R197A	4.3 (±0.1)	125 (±28)	288 (±4)	185 (±69)	600 (±10)	1.37 (±0.25)	6.66 (±0.68)

[a] The values of the parameters were obtained by fitting the data for the first phase shown in Figure 5 to eq 2 as described under Experimental Procedures. The values of k_0 were determined by linear extrapolation to zero of the data for k_{obs} at very low ATP concentrations, where k_{obs} is ATP concentration-independent. These values were used as constants in the data fitting. Single-letter notation for amino acids is used.

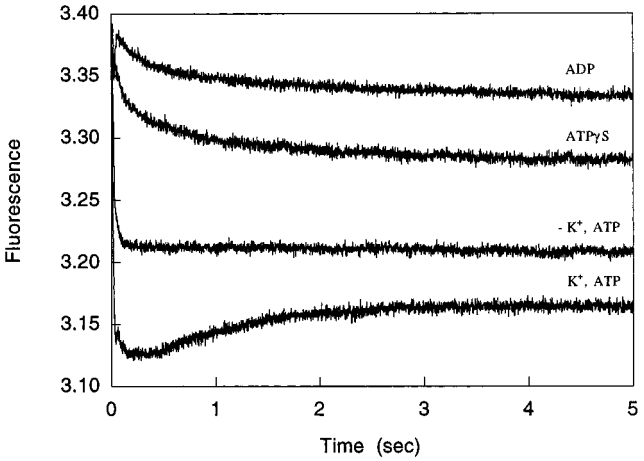

FIGURE 6: Time-resolved change in fluorescence emission upon rapid mixing of GroEL with ADP, ATPγS, and ATP with or without 10 mM K^+. Equal volumes of the Phe44 → Trp mutant GroEL and ADP, ATPγS, or ATP in the presence of 10 mM K^+, or ATP in the absence of K^+,were rapidly mixed, and the time-resolved change in fluorescence emission upon excitation at 280 nm was followed. The adenine nucleotide concentration was 400 μM, and the oligomer concentration of the Phe44 → Trp GroEL mutant was 125 nM. For further details see Experimental Procedures.

for ATP (*8*, *24*). Second, recent cryoelectron microscopy studies have shown differences between the conformations of unliganded and ADP- and ATP-bound forms of GroEL rings (*16*). The largest differences in conformation are between the unliganded state and adenine nucleotide-bound states, but there are also some differences in conformation between the ADP- and ATP-bound forms. Third, differential effects of ADP and ATP on GroEL-mediated folding of tryptophanase have been observed, suggesting that they stabilize different conformations of GroEL (*25*).

The Third Phase Reflects the Presence of Residual Contaminants. The value of the rate constant corresponding to this phase is between 1 and 3 s^{-1}, and it has a weak sigmoidal dependence on ATP concentration. A single-exponential phase with a similar rate constant and small amplitude is observed when wild-type GroEL (which has no tryptophan residues) is mixed with ATP and fluorescence emission is monitored upon excitation at 295 nm with a band-pass of 4.65 nm (not shown). A single-exponential phase with a similar rate constant but a 10-fold larger amplitude is observed when ATP is mixed with less clean wild-type GroEL, which was purified according to our standard protocol but without the additional methanol step. This phase is thus due to the presence of residual contaminants in our GroEL preparations, which contain not more than 1 mol of tryptophan/mol of GroEL oligomer (*15*). A similar single-exponential phase is observed also when wild-type GroEL is rapidly mixed with ATP in the absence of K^+. The contaminants are, therefore, not acting as a probe for the transition of GroEL from an ATP-bound state to an ADP-bound state. This phase, therefore, probably reflects the ATP-dependent release of residual contaminants from GroEL. The rate constant corresponding to this phase is similar to that of dissociation of modified horse cytochrome *c* from GroEL (*26*).

DISCUSSION

A bi-sigmoidal dependence on ATP concentration of the observed rate constant of ATP binding-induced conformational changes in GroEL is here reported for the first time. A bi-sigmoidal dependence of the observed rate constant of polypeptide substrate dissociation from GroEL on ATP concentration has been reported (*27*). In a previous stopped-flow study of ATP binding to GroEL using a pyrene maleimide probe (*8*), a simple hyperbolic dependence on ATP concentration was observed, probably owing to the relatively high concentrations of ATP and GroEL employed in that study. The study by Jackson et al. (*8*) supports, however, the assumptions made here, namely, that ATP binding is fast relative to the main conformational change and that the reverse conformational changes can be neglected. Here, two additional kinetic phases are observed which reflect (i) the transition from the ATP-bound state of GroEL to the ADP-bound state and (ii) the presence of bound contaminants. These phases were not reported by Jackson et al. (*8*), but in the more recent study by Burston et al. (*28*) an ATP hydrolysis phase was observed which has a rate constant that is very similar to the one found in this study. This rate constant probably corresponds to hydrolysis of ATP to ADP−P_i and not to the release of inorganic phosphate, which is measured in the steady-state experiments (Figure 3).

In previous steady-state experiments (*20*), the mutation Arg197 → Ala was found to reduce the value of the Hill coefficient of the first allosteric transition to ~1 but have little effect on the intrinsic affinity of ATP for GroEL. The values of the Hill coefficients for the first allosteric transition of the Phe44 → Trp single mutant and the Phe44 → Trp; Arg197 → Ala double mutant, here obtained from the transient kinetic data, are strikingly similar to those determined in steady-state experiments (Figure 2; ref 10). Taken together, these results indicate that the first phase reflects a conformational transition in GroEL induced by ATP binding. The values of the Hill coefficients for the second transition, determined here from transient kinetic data, are ~7, reflecting the strong negative cooperativity between rings and suggesting that the second transition may occur in an all-or-none fashion. Negative cooperativity between rings with respect to ATP binding is also reflected in the finding that $K_1 < K_2$.

In accordance with the MWC model, the rank order of values of the rate constants of conformational changes for both mutants is $k_2 > k_1 > k_0$, indicating that bound ATP facilitates the allosteric transition. In the presence of the mutation Arg197 → Ala, the values of k_0, k_1, and k_2 are all larger, consistent with the conclusion from steady-state studies that this mutation shifts the equilibrium toward the **TR** and **RR** states (*20*). In the presence of ATP, the rate of the conformational change is >100 s^{-1}, whereas in the absence of ATP it is ~ 0.7 s^{-1}. The rate of the reverse conformational change of the Phe44 → Trp mutant in the absence of ATP is, therefore, calculated to be ~ 350 s^{-1}. The forward rates of allosteric transitions are similar to those of *E. coli* phosphofructokinase (*29*) and aspartate transcarbamylase (*30*) and are slower than those of hemoglobin (*31*). The rate of folding of proteins, such as barnase, which fold relatively quickly, is ~ 10 s^{-1} (*32*). In the presence of ATP, the rates of the allosteric changes in GroEL are at least 1 order of magnitude faster than such rates of protein folding. Owing to this large difference, the actual folding process under such circumstances will be kinetically uncoupled to the conformational changes in GroEL. In the absence of ATP, the rate of conformational changes in GroEL is much slower, which may explain why the folding of some proteins, such as barnase, is retarded in the presence of GroEL when ATP is absent (*33*).

REFERENCES

1. Braig, K., Otwinowski, Z., Hegde, R., Boisvert, D. C., Joachimiak, A., Horwich, A. L., and Sigler, P. B. (1994) *Nature 371*, 578−586.
2. Braig, K., Adams, P. D., and Brünger, A. T. (1995) *Nat. Struct. Biol. 2*, 1083−1094.
3. Ellis, R. J., and Hartl, F.-U. (1996) *FASEB J. 10*, 20−26.
4. Fenton, W. A., and Horwich, A. L. (1997) *Protein Sci. 6*, 743−760.
5. Horovitz, A. (1998) *Curr. Opin. Struct. Biol. 8*, 93−100.
6. Gray, T. E., and Fersht, A. R. (1991) *FEBS Lett. 292*, 254−258.
7. Bochkareva, E. S., Lissin, N. M., Flynn, G. C., Rothman, J. E., and Girshovich, A. S. (1992) *J. Biol. Chem. 267*, 6796−6800.
8. Jackson, G. S., Staniforth, R. A., Halsall, D. J., Atkinson, T., Holbrook, J. J., Clarke, A. R., and Burston, S. G. (1993) *Biochemistry 32*, 2554−2563.
9. Todd, M. J., Viitanen, P. V., and Lorimer, G. H. (1993) *Biochemistry 32*, 8560−8567.
10. Yifrach, O., and Horovitz, A. (1995) *Biochemistry 34*, 5303−5308.
11. Monod, J., Wyman, J., and Changeux, J.-P. (1965) *J. Mol. Biol. 12*, 88−118.
12. Yifrach, O., and Horovitz, A. (1996) *J. Mol. Biol. 255*, 356−361.
13. Koshland, D. E., Jr., Némethy, G., and Filmer, D. (1966) *Biochemistry 5*, 365−385.
14. Kovalenko, O., Yifrach, O., and Horovitz, A. (1994) *Biochemistry 33*, 14974−14978.
15. Inbar, E., and Horovitz, A. (1997) *Biochemistry 36*, 12276−12281.
16. Roseman, A. M., Chen, S., White, H., Braig, K., and Saibil, H. R. (1996) *Cell 87*, 241−251.
17. White, H. E., Chen, S., Roseman, A. M., Yifrach, O., Horovitz, A., and Saibil, H. R. (1997) *Nat. Struct. Biol. 4*, 690−694.
18. Llorca, O., Marco, S., Carrascosa, J. L., and Valpuesta, J. M. (1997) *J. Struct. Biol. 118*, 31−42.
19. Horovitz, A., Bochkareva, E. S., Kovalenko, O., and Girshovich, A. S. (1993) *J. Mol. Biol. 231*, 58−64.
20. Yifrach, O., and Horovitz, A. (1994) *J. Mol. Biol. 243*, 397−401.
21. Viitanen, P. V., Lubben, T. H., Reed, J., Goloubinoff, P., O'Keefe, D. P., and Lorimer, G. H. (1990) *Biochemistry 29*, 5665−5671.
22. Hammes, G. G., and Schimmel, P. R. (1966) *J. Phys. Chem. 70*, 2319−2324.
23. Hammes, G. G. (1968) *Adv. Protein Chem. 23*, 1−57.
24. Corrales, F. J., and Fersht, A. R. (1996) *Proc. Natl. Acad. Sci. U.S.A. 93*, 4509−4512.
25. Mizobata, T., Akiyama, Y., Ito, K., Yumoto, N., and Kawata, Y. (1992) *J. Biol. Chem. 267*, 17773−17779.
26. Hoshino, M., Kawata, Y., and Goto, Y. (1996) *J. Mol. Biol. 262*, 575−587.
27. Lin, Z., and Eisenstein, E. (1996) *Proc. Natl. Acad. Sci. U.S.A. 93*, 1977−1981.
28. Burston, S. G., Ranson, N. A., and Clarke, A. R. (1995) *J. Mol. Biol. 249*, 138−152.
29. Auzat, I., Gawlita, E., and Garel, J.-R. (1995) *J. Mol. Biol. 249*, 478−492.
30. Hammes, G. G., and Wu, C.-W. (1971) *Biochemistry 10*, 1051−1057.
31. Martino, A. J., and Ferrone, F. A. (1989) *Biophys. J. 56*, 781−794.
32. Matouschek, A., Serrano, L., and Fersht, A. R. (1992) *J. Mol. Biol. 224*, 819−835.
33. Gray, T. E., and Fersht, A. R. (1993) *J. Mol. Biol. 232*, 1197−1207.

BI980370O